Short Communication

Combining reverse end-to-side neurorrhaphy with rapamycin treatment on chronically denervated muscle in rats

Yijian Chen[1,†], Wanqiong Yuan[2,†], Xiaolong Zeng[1,†], Yuanchen Ma[1], Qiujian Zheng[1], Bofu Lin[1], Qingtian Li[1,*]

[1] *Department of Orthopedics, Guangdong Provincial People's Hospital, Guangdong Academy of Medical Sciences, 510000 Guangzhou, Guangdong, China*

[2] *Department of Orthopedics, Peking University Third Hospital, Beijing Key Laboratory of Spinal Disease, 100044 Beijing, China*

*Correspondence: liqingdian@gdph.org.cn (Qingtian Li)
† These authors contributed equally.

DOI:10.31083/j.jin2002035

Submitted: 4 February 2021 Revised: 4 March 2021 Accepted: 7 April 2021 Published: 30 June 2021

This preliminary research determines whether a combination of reverse end-to-side neurorrhaphy and rapamycin treatment achieves a better functional outcome than a single application after prolonged peripheral nerve injury. We found that the tibial nerve function of the reverse end-to-side + rapamycin group recovered better, with a higher tibial function index value, higher amplitude recovery rate, and shorter latency delay rate ($P < 0.05$). The reverse end-to-side + rapamycin group better protected the gastrocnemius muscle with more forceful contractility, tetanic tension, and a higher myofibril cross-sectional area ($P < 0.05$). Combining reverse end-to-side neurorrhaphy with rapamycin treatment is a practical approach to promoting the recovery of chronically denervated muscle atrophy after peripheral nerve injury.

Keywords

Peripheral nerve injury; Muscle denervation; Nerve regeneration; Reverse end-to-side neurorrhaphy; Rapamycin

1. Introduction

Peripheral nerve injury frequently leads to poor functional recovery, particularly when nerve regeneration is adjourned and/or the injury is far from the target organ [1, 2]. Poor recovery should be attributed to irreversible atrophy of the target muscle [3, 4]. After severe nerve injury, the speed of nerve regeneration is usually limited, leading to nerve denervation of the target muscle for a long time. An effective connection of the nerve with the target muscle has failed skeletal muscle atrophy [5–8]. Therefore, it is necessary to prevent target muscle atrophy by improving the repair of severe nerve injury.

One solution is the early nerve protection technique for the denervated muscle, namely the traditional end-to-side (ETS) neurorrhaphy technique. This technique consists of transecting the distal stump and then suturing on an adjacent nerve in end-to-side form. Then the ETS neurorrhaphy is transected, and the distal stump is sutured to the proximal stump in an end-to-end fashion after the proximal stump reaches the distal stump [7–11]. Although these methods can provide innervation for the target muscle before the original axon reaches the distal nerve stump, the stumps undergo Waller degeneration twice before reinnervation by the natural axon, which adversely affects axon regeneration and functional recovery [12]. As a development of this technique, we designed the reverse end-to-side (RETS) neurorrhaphy technique. An epineural window on a distal nerve stump is created in suture with an adjacent nerve in RETS fashion in the RETS procedure. The RETS nerve transfer provides supplementary motor axons to enhance regenerative nerve and supplies early motor endplate reinnervation, protecting the target organs until the original intrinsic axon regeneration has occurs. Previous studies have shown that the RETS technique effectively prevented denervated muscle atrophy and significantly improved the functional outcome in rats [13–15].

Recent studies showed that the mammalian target of rapamycin (Ra) complex 1 (mTORC1) plays a vital role in protein degradation and leads to muscle atrophy following denervation [16–20]. After the denervation of skeletal muscle, mTORC1 upregulates the phosphorylation of protein kinase B (PKB)/Akt, which increases the expression of transcription factor forkhead box O (FoxO), muscle-specific E3 ubiquitin ligases atrogin-1 (muscle atrophy F-box protein, MAFbx) and muscle-specific ring finger 1 (MuRF1). It accelerates denervation muscle atrophy [16, 21, 22]. Tang's group found that the mTORC1-FoxO pathway was inhibited in denervated skeletal muscle by the inhibitor of mTORC1: Ra, which improved the outcomes of denervated gastrocnemius muscle atrophy [23–26]. These studies suggested that rapamycin could improve the denervated muscle recovery after suffering from peripheral nerve injury.

Irreversible muscle atrophy caused by chronic denervation is the main reason for poor functional recovery following severe nerve injury. We have previously proven that the reverse end-to-side neurorrhaphy technique prevented denervated muscle atrophy and improved the functional outcome [13–15]. Recent studies indicated the protective effect for denervated muscle atrophy with the treatment of rapamycin [24]. The present study tests the hypothesis that a combination of RETS neurorrhaphy and rapamycin treatment will improve the functional outcome of chronic denervation muscle after peripheral nerve injury has occurred.

Journal of Integrative Neuroscience

2. Methods

2.1 Animals

Adult female Sprague-Dawley rats (eight weeks, 200–250 g) were used in the present study. Rats were housed under controlled, pathogen-free conditions, 12/12-hour light/dark cycle with free access to pellet food and water.

2.2 Group

Rats were randomly grouping into four groups (n = 6 each): the denervation with control cosolvent treatment group (Den group), RETS protection with control cosolvent treatment group (RETS group), denervation with rapamycin treatment group (Den + Ra group) and RETS protection with rapamycin treatment group (RETS + Ra group).

2.3 Surgical procedures

2.3.1 Tibial nerve injury

The right hind limb of each animal was operated with an aseptic technique. Briefly, adult rats were anesthetized with sodium pentobarbital (30 mg/kg) by intraperitoneal injection. After removing fur, povidone-iodine was used to disinfect the local skin. A parallel longitudinal incision was made from the hip to the posterior femur, exposing the sciatic nerve from proximal to trifurcation and freeing the tibial, peroneal and sural nerves completely. The denervation was performed as per the following processes: the tibial nerve was cut 6.5 mm away from the proximal part of the tibial nerve into the gastrocnemius muscle. The nerve stumps were covered with a silicone cap [27] to prevent natural reinnervation (Fig. 1A,C). For the groups of RETS protection in the base of denervation, and epineurium window was set up on the distal stump 3.5 mm away from the position of the tibial nerve entering into the gastrocnemius muscle, 40% of the peroneal nerve on the horizontal level of the transverse of the tibial nerve was separated, and the proximal stump of peroneal nerve was sutured at the epineural window in RETS neurorrhaphy (Fig. 1B,D). Four weeks after the initial surgery, all rats had performed a second surgery by removing the distal and proximal tibial stumps, trimming the scar and suturing two stumps together in an end-to-end (ETE) neurorrhaphy. The surgical wounds of all animals were thoroughly rinsed and closed in layers until the wounds healed.

2.3.2 In-vivo rapamycin treatment of rats

The rats were treated with rapamycin (LC Laboratories) or control cosolvent by intraperitoneal injection after the first surgery and terminated eight weeks after the second surgery. Rapamycin was dissolved at 20 mg/mL in ethanol and stored at -20 °C. The stored solution was diluted with 5% Tween 80 (Sigma), 5% polyethylene glycol 400 (Sigma), and axenic saline solution immediately before usage. Rats were administered 6 mg/kg rapamycin by intraperitoneal injection twice weekly. The same cosolvent without rapamycin was used in the control group [28].

2.4 Tibial function index analysis

Tibial Function Index (TFI) analysis was performed after the second operation. Animals were allowed to walk on a closed footpath (10 cm × 60 cm) every two weeks, with the bottom covered with white paper. The rats' hind limbs were dipped in black ink before putting them on the inlet port of the footpath to initiate movement. At the end of the test, clear and complete footprints were used to measure the following parameters. The print length (PL; heel to toe distance), toe extension (TS; first to fifth toe distance), and middle toe extension (IT; second to fourth toe distance) were recorded as paired footprint parameters. The normal hind limb (NPL, NTS, and NIT) and the experimental hind limb (EPL, ETS, and EIT) were set as controls and experimental feet. Finally, we used the Bain MacKinnon Hunter formula to calculate the TFI index: TFI = -37.2 ([EPL-NPL]/NPL) + 104.4 ([ETS-NTS]/NTS) + 45.6 ([EIT-NIT]/NIT) - 8.8 [29].

2.5 Electrophysiology

The electrophysiological test was performed by computer-aided electromyography (EMG) and a nerve conduction velocity system (NC-STAT; NeuroMetrix, Japan). The rats' experimental and healthy sides' tibial nerves were exposed eight weeks after the second surgery. Then electrical stimuli (Intensity 5 V, duration 0.1 ms, frequency 1 Hz) were performed on the tibial nerve stem 3.5 mm proximally away from the tibial nerve. The recording electrodes were placed 2 mm proximally and distally away from the repair point of the tibial nerve to measure the Compound Muscle Action Potentials (CMAP) (Fig. 2). After recording the latency and amplitude, the latency delay rate (LDR) and the amplitude recovery rate (ARR) for each rat were calculated to compare the latency and CMAP of the surgical and contralateral control side.

2.6 Muscle contractile force

The twitch and tetanic tensions of the gastrocnemius muscle were used to show the recovery of muscle strength. After completing of the electrophysiology, the gastrocnemius muscle was exposed and separated from the surrounding tissues with intact tibial nerve. The hind limbs were constrained with forceps, then the distal tendon of the gastrocnemius muscle was connected to a force sensor through a nylon ligature. 50 Hz electrical stimulation was used for tonic tension. The testing was conducted with a force sensor (JZJ101; Guangzhou Instrument Factory, Guangdong, P.R. China) and a computerized bioelectric signal processing system (SMUP-E; Guangdong General Hospital, Guangdong, P.R. China).

2.7 Muscle wet weight

The gastrocnemius muscle with the tibial nerve was freed completely after testing the muscle force. The wet muscle weight was scaled by analytical balance (BSA124S, sartorius). The measurement of the surgical side was compared with the contralateral side and recorded the ratio to show the retention of the wet muscle weight.

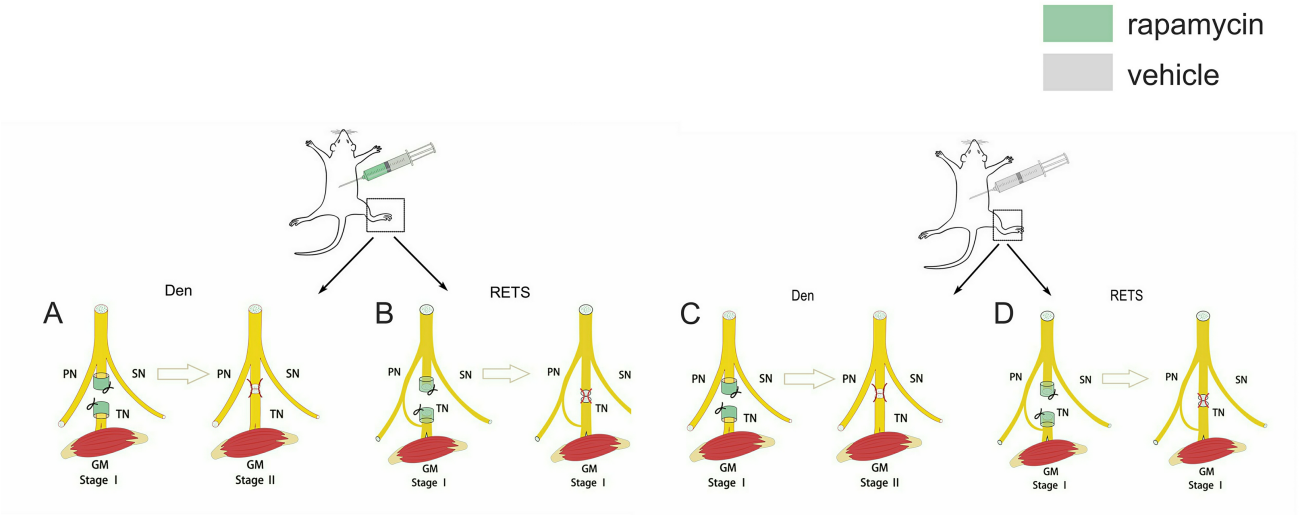

Fig. 1. Schematic diagram of surgical procedures for gastrocnemius muscle (GM) of the right hind limb of rats and intraperitoneal treatment with rapamycin or carrier in rats. Gastrocnemius denervation with rapamycin treatment (A); Gastrocnemius denervation with 40% of peroneal nerve RETS neurorrhaphy protection and rapamycin treatment (B); Gastrocnemius denervation with control cosolvent treatment (C); Gastrocnemius muscle denervation with 40% of peroneal nerve reverse end-to-side neurorrhaphy protection and vehicle treatment (D). TN, tibial nerve; GM, gastrocnemius muscle; PN, peroneal nerve; SN, sural nerve; Stage II, four weeks after Stage I.

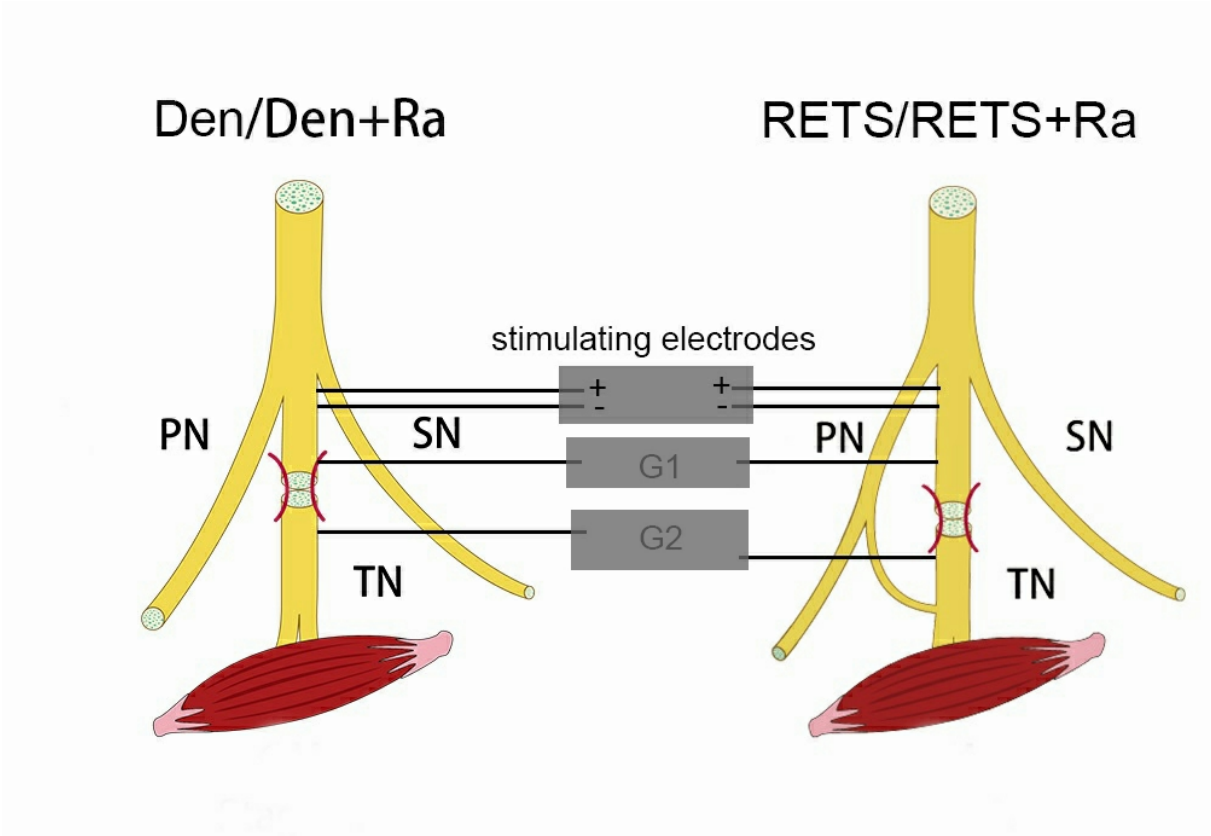

Fig. 2. The electrophysiology tests of the gastrocnemius muscle. The stimulating electrode (Intensity 5 V, duration 0.1 ms, frequency 1 Hz) was placed on the tibial nerve trunk at 3.5 mm proximal of the tibial nerve. The recording electrodes (G 1, G 2) were 2 mm proximally and distally away from the repair point of the tibial nerve. TN, tibial nerve; PN, peroneal nerve; SN, sural nerve; GM, gastrocnemius muscle.

2.8 Morphological evaluation and cross-sectional muscle measurement

After weighing, the gastrocnemius muscle was divided into several parts. One of the samples was dehydrated through graded ethanol, clarified with xylene, embedded with paraffin, then sliced at four μM. After H&E staining, the muscle fibers' cross-sectional area was recorded with a dfc300fx color digital camera (Leica). Four random fields from three sections in every specimen (Leica Q550 IW; Leica Imaging Systems Ltd.) were taken for analysis with Leica QWin software (Leica Imaging Systems Ltd.).

2.9 Statistical analysis

Data were analyzed with SPSS 26.0 software (SPSS Inc.). Statistical analysis was performed using two-tailed Student's *t*-tests to compare differences between two groups. One-way analysis of variance (ANOVA) was used for experiments that required comparing between three or more groups, including a Tukey's post-hoc test. For all experiments, results were considered significant at $P < 0.05$ (*), $P < 0.01$ (**) and $P < 0.001$ (***), and values are presented as the mean ± standard deviation (SD).

3. Results

3.1 General observations

There were no systemic or local inflammation or postoperative complications after experiments in rats. No automutilation was found in the experiment. The motor function of each group recovered gradually.

3.2 Tibial function index analysis

TFI analysis showed that the TFI values of the four groups decreased after denervation, and gradually increased after the tibial nerve repair (Fig. 3). The TFI values in the Den + Ra group were significantly higher than in the Den group at every time point ($P < 0.001$, Fig. 3). The TFI values in the RETS group were significantly higher than in the Den group at every time point ($P < 0.001$, Fig. 3). The TFI values in the RETS + Ra group were significantly higher than in the Den group at every time point ($P < 0.001$, Fig. 3). The TFI values in the RETS group were significantly lower than in the RETS + Ra group at every time point ($P = 0.014$, 6 weeks after the first surgery, $P < 0.001$, 8, 10, 12 weeks after the first surgery, Fig. 3). The TFI values in the Den + Ra group were significantly lower than the RETS + Ra group at every time point ($P < 0.001$, Fig. 3).

3.3 LDR and ARR

The results of the LDR and AAR of the gastrocnemius muscle are displayed in Fig. 4. The AAR in RETS + Ra reached 0.68, significantly higher than those of the other three groups ($P < 0.001$, Fig. 4A). The RETS protection group showed higher ARR (0.53) than that of the Den + Ra group (0.36) ($P = 0.001$, Fig. 4A). The denervation group showed poor recovery in amplitude, where the ARR only amounted to 0.07.

The LDR in the denervation and Den + Ra groups reached 2.93 and 3.22, respectively, and these were not significantly different ($P = 0.234$, Fig. 4B). However, the LDR in the Den and Den + Ra groups was worse than the RETS + Ra group and the RETS protection group (1.54, 2.20, $P < 0.001$, Fig. 4B). The LDR in the RETS + Ra group was higher than the RETS protection group ($P = 0.008$, Fig. 4B).

3.4 Muscle contractile force

The measurements of contractile force included twitch and tetanic tension. The twitch tension of the gastrocnemius muscle with RETS + Ra protection reached 1.68 ± 0.03 N, which was significantly stronger than that of any of the other groups ($P < 0.001$, Fig. 5A). The twitch tension in the RETS protection group (1.13 ± 0.02 N) was greater than that in the Den + Ra group. The twitch tension was worst in the denervation group, significantly different from the other three groups (0.85 ± 0.04 N, $P < 0.001$, Fig. 5A). A similar performance was performed for tetanic tension. It was significantly stronger than other groups: the RETS + Ra protection group (5.17 ± 0.01 N, $P < 0.001$, Fig. 5B), followed by the RETS protection group (3.81 ± 0.04 N), the Den + Ra group (2.98 ± 0.02 N) and the denervation group (1.77 ± 0.02 N). Pairwise comparisons among the four groups were statistically significant ($P < 0.001$, Fig. 5B).

3.5 Muscle wet weight

The ratio calculated the result of wet muscle weight: surgical side/contralateral side and the results are shown in Fig. 5C. The wet weight of the surgical side of the RETS + Ra group was nearly completely retained (0.96), which was statistically significant compared to the other three groups ($P < 0.001$, Fig. 5C). The ratios were 0.78 and 0.73 in the RETS protection group and the Den + Ra group, respectively. There were no statistically significant differences between the RETS and the Den + Ra group ($P = 0.089$, Fig. 5C). As previously reported, the retention of the denervation group presented the worst among the four groups (0.62, $P < 0.001$, Fig. 5C).

3.6 Evaluation of the gastrocnemius muscle ultrastructure

The ultrastructure of the gastrocnemius muscle in the four groups is shown in Fig. 6. It can be observed that the ultrastructure of the gastrocnemius muscle in the four groups was generally preserved, but all groups showed varying degrees of fibrous connective tissue hyperplasia. The myofibril cross-sectional area in the RETS + Ra group was 2234.19 ± 671.59 μm^2, which was twice as large as that in the denervation group (1119.42 ± 260.79 μm^2, $P < 0.001$, Fig. 6). The RETS protection group (1510.40 ± 350.93 μm^2) was not statistically different from the Den + Ra group (1428.94 ± 327.69 μm^2, $P = 0.348$, Fig. 6).

4. Discussion

Functional recovery has been disappointing in peripheral nerve injury, particularly when nerve regeneration is adjourned and/or the injury is far from their target organs [1]. Due to the limited speed of nerve regeneration in se-

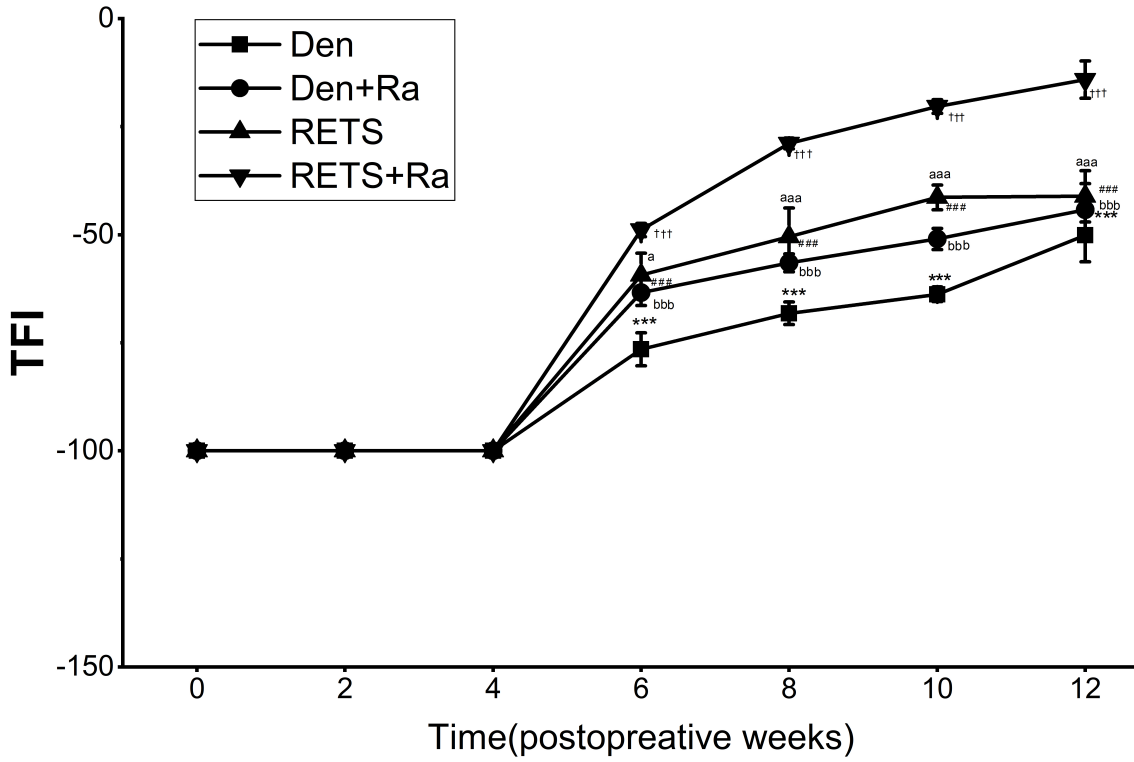

Fig. 3. The tibial function index was determined after analysis of the walking trajectory. The higher the TFI score, the better the functional recovery. *Den group versus Den + Ra group, #Den group versus RETS group, † Den group versus RETS + Ra group, a Den + Ra group versus RETS + Ra group, b RETS group versus RETS + Ra group. Results statistically significant at $P < 0.05$ (*, #, †, a, b), $P < 0.01$ (**, ##, ††, aa, bb) and $P < 0.001$ (***, ###, †††, aaa, bbb).

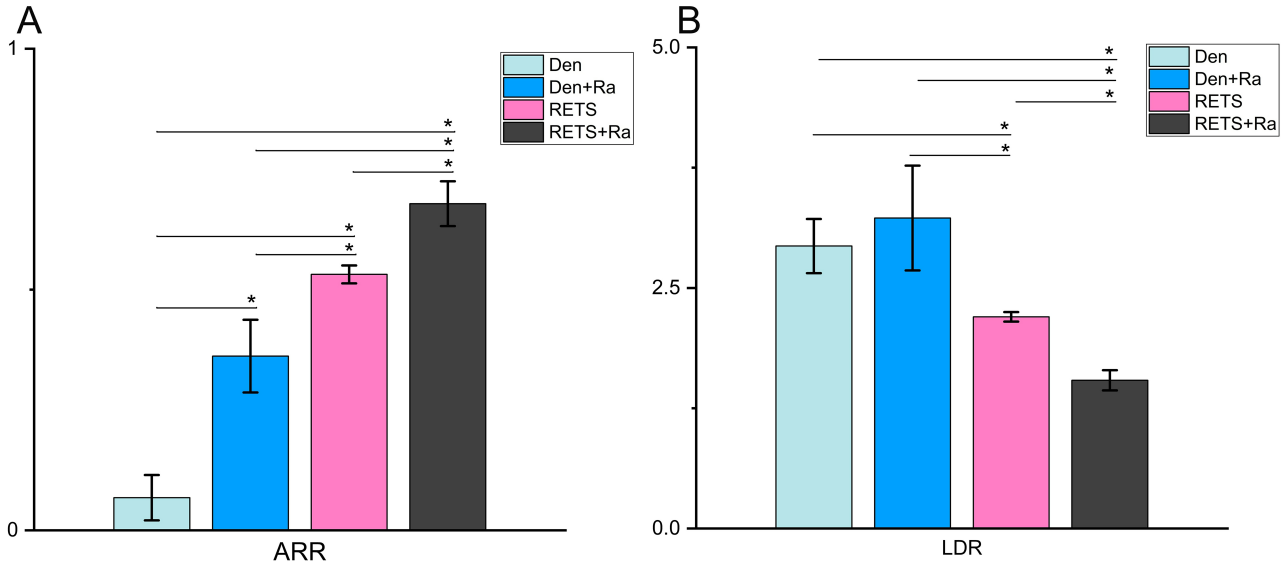

Fig. 4. The LDR and ARR of each rat were determined by calculating surgical side results divided by the contralateral side. AAR of the gastrocnemius muscle (A); LDR of the gastrocnemius muscle (B). Results statistically significant at $P < 0.05$ (*).

vere nerve injury, it takes months or even a year for axons to reach the target organ. The denervated skeletal muscle may have atrophied or developed fibrosis, even though the axon has regenerated [2, 6]. An effective connection with the atrophied muscle may have failed, which results in poor functional outcomes in peripheral nerve injury [6, 30, 31]. Therefore, protecting the target muscles from chronic denervation may be an essential strategy in improving the functional outcome after peripheral nerve injury. The present study explored the therapeutic potential of combining RETS

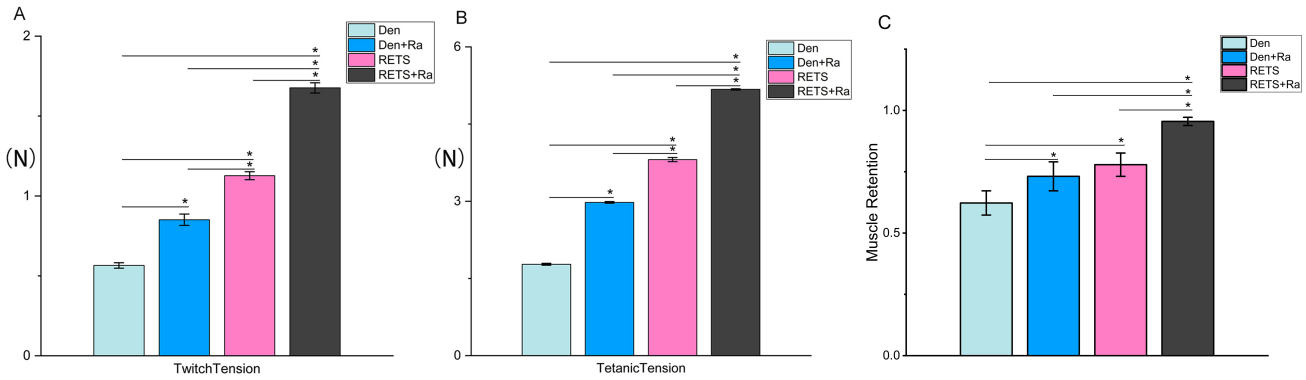

Fig. 5. Measurement of gastrocnemius contractility. Convulsive tension (A); tonic tension (B). The ratio of the gastrocnemius muscle mass on the surgical side to the healthy side (C). Results statistically significant at $P < 0.05$ (*).

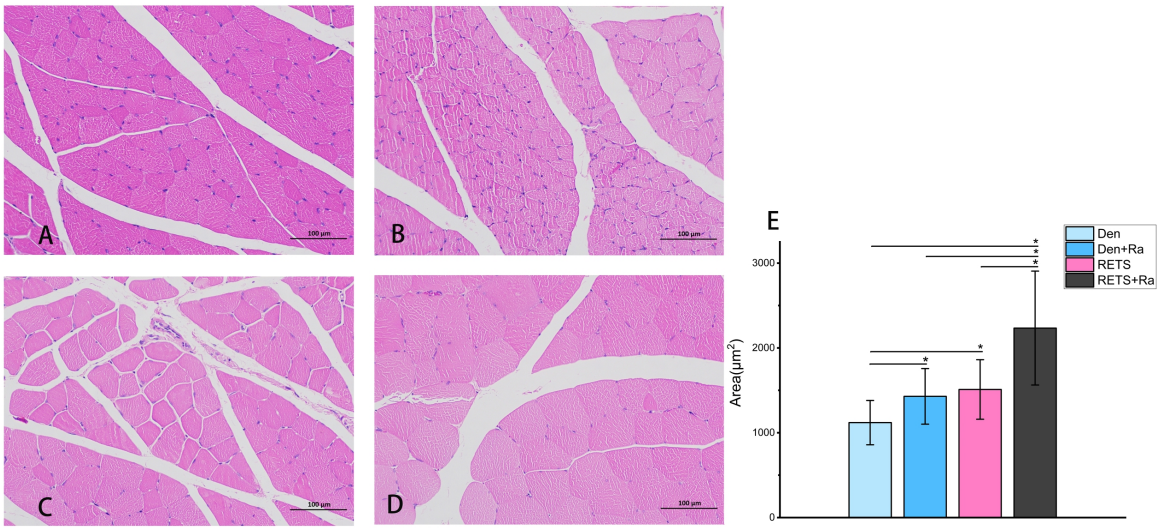

Fig. 6. H&E staining cross-section micrographs of gastrocnemius muscle in four groups. Denervation group (A); Den + Ra group (B); RETS nerve protection group (C); RETS + Ra group (D); Original magnification × 200; bar = 100 μm. Measurements of cross-sectional area on gastrocnemius muscle at 12 weeks (E). Results statistically significant at $P < 0.05$ (*).

and rapamycin treatment by using the model of chronic denervation in the gastrocnemius muscle of rats. We proved that the combination of RETS and rapamycin treatment achieved better functional results concerning the chronic denervation model of rats than the single application. Among the four groups, the tibial nerve function of the RETS + Ra group recovered better, with a higher TFI value, higher ARR, and shorter LDR. Furthermore, RETS + Ra provided better protection for the gastrocnemius muscle, stronger muscle contractility and tetanic tension, and a higher myofibril cross-sectional area.

In the traditional ETS neurorrhaphy technique, an adjacent nerve is partially transected then sutured to the distal stump of the injured nerve in ETE form to provide early protection. However, the distal nerve stump undergoes Waller degeneration twice before reinnervation by the natural axon, affecting axon regeneration and functional recovery [12]. Recently, we developed the traditional ETS neurorrhaphy technique into RETS [14]. The RETS technique allows the injured nerve to re-innervate with the adjacent nerve suture on the perineurial window of the chronically denervated distal nerve stump [14, 15]. Likely, that the anterior interosseous nerve (AIN) transfer techniques in treating cubital tunnel syndrome achieve good results clinically [32]. Previous studies found it was better to choose a mixed nerve as a donor's nerve because it complements the motor axons required to promote functional recovery of the denervated muscle [13]. It indicated that the ETS neurorrhaphy technique procedure using a donor nerve with a partial neurectomy of 40% was the best choice for effectually treating peripheral nerve injury in rats [33]. Therefore, it is reasonable in this study to separate and suture 40% of the peroneal (mixed) nerve at the epineural window that was set up on the distal stump 3.5 mm away from the position of the tibial nerve

entering into the gastrocnemius muscle in the form of RETS neurorrhaphy. The results of TFI, ARR and LDR showed that the recovery of tibial nerve function in the RETS group was significantly higher than in the denervated group, which indicated more rebuild of intact nerve-muscle contacts. The ability of nerves with intact nerve-endplate connection to increase the number of muscle fibers in denervated muscles is 5–8 times greater than that of impaired nerves [34, 35]. It is consistent with the myofibril cross-sectional area and muscle wet weight retention in the RETS group. These partially denervated muscles fully recovered their contractile strength with good protective effects on chronically denervated muscle atrophy.

The essence of denervated muscle atrophy results from more significant muscle protein degradation than synthesis [36–38]. The mTORC1, one of the effectors that play an essential role in protein regulation, has been identified as being strongly activated after denervation [21, 39, 40]. Tang *et al.* [24] showed that mTORC1-FoxO-E3 ubiquitin ligase cascade was activated after denervation, which led to muscle atrophy [26]. By using rapamycin, this "atrophy cascade" was inhibited, and the target muscle was rescued. In this study, the rapamycin treatment group had a larger cross-sectional area and muscle mass retention than the denervation group. The recovery of nerve function in the rapamycin treatment group was better than that of the denervation group. Castets's finding could explain these results [41]. After skeletal muscle denervation, PKB/Akt inhibition, conferred by sustained mTORC1 activation, abrogated denervation-induced synaptic remodeling and caused neuromuscular endplate degeneration, which could be reversed by rapamycin.

Of course, there are some limitations to this study. Here, we just chose part of the peroneal nerve as a donor's nerve. However, whether RETS can be applied to other nerves still needs more investigation. Furthermore, although we have proven that rapamycin was beneficial to prevent denervated skeletal muscle atrophy, the treating time, optimal dose, and frequency and duration of rapamycin treatment are still uncertain, which needs further studies.

5. Conclusions

In conclusion, our study demonstrates the potential for a combination approach including RETS and rapamycin in treating chronically denervated muscle. The effect of the RETS neurorrhaphy technique combined with rapamycin was significantly better than that of RETS or rapamycin alone. This combination of surgery and drug therapy could provide a new approach to treating peripheral nerve injury.

Abbreviations

RETS, reverse end-to-side; Ra, rapamycin; ETS, end-to-side; mTORC1, mammalian target of rapamycin (Ra) complex 1; PKB, protein kinase B; FoxO, factor forkhead box O; MAFbx, muscle atrophy F-box protein; MuRF1, muscle-specific ring finger 1; Den, denervation; ETE, end-to-end; TFI, Tibial Function Index; PL, print length; TE, toe extension; IT, middle toe extension; NPL, normal print length; NTE, normal toe extension; NIT, normal middle toe extension; EPL, experimental print length; ETE, experimental toe extension; EIT, experimental middle toe extension; EMG, electromyography; AIN, anterior interosseous nerve; CMAP, Compound Muscle Action Potentials; LDR, Latency Delay Rate; ARR, Amplitude Recovery Rate; ANOVA, One-way analysis of variance; SD, standard deviation.

Author contributions

QL designed this study. YC and XZ carried out the study and collected the data. YC, WY and BL drafted the manuscript. YM and QZ made critical suggestions for this study. All authors approved the final manuscript.

Ethics approval and consent to participate

All work was performed in accordance with the Guiding Opinions on the Treatment of Experimental Animals, Guangdong Province Laboratory Animal Management Regulations and the Laboratory Animal Committee (LAC) of the South China University of Technology Policy on the Humane Care and Use of Vertebrate Animals. Ethics approval was obtained from the Administration Committee of the Guangdong Provincial People's Hospital, Guangdong Academy of Medical Sciences (Permit Number: 2018537A).

Acknowledgment

We thank Wenhan Huang for his assistance in manuscript preparation.

Funding

This project is supported by the Major Science and Technology Project of Guangdong Province (2015B020225007), Natural Science Foundation of Guangdong Province (2018A0303130206, 2021A1515011008), Guangdong Medical Science and Technology Research Fund (A2019150), and the Program of Science and Technology of Guangzhou (201904010424).

Conflict of interest

The authors declare no conflict of interest.

References

[1] Midha R. Epidemiology of brachial plexus injuries in a multitrauma population. Neurosurgery. 1997; 40: 1182–1189.

[2] Huckhagel T, Nüchtern J, Regelsberger J, Lefering R; TraumaRegister DGU. Nerve injury in severe trauma with upper extremity involvement: evaluation of 49,382 patients from the TraumaRegister DGU® between 2002 and 2015. Scandinavian Journal of Trauma, Resuscitation and Emergency Medicine. 2018; 26: 76.

[3] Höke A, Gordon T, Zochodne DW, Sulaiman OA. A decline in glial cell-line-derived neurotrophic factor expression is associated with impaired regeneration after long-term Schwann cell denervation. Experimental Neurology. 2002; 173: 77–85.

[4] Gordon T, Tyreman N, Raji MA. The basis for diminished func-

tional recovery after delayed peripheral nerve repair. Journal of Neuroscience. 2011; 31: 5325–5334.
[5] Kalantarian B, Rice D, Tiangco D, Terzis J. Gains and losses of the XII-VII component of the "baby-Sitter" procedure: a morphometric analysis. Journal of Reconstructive Microsurgery. 1998; 14: 459–471.
[6] Aydin MA, Mackinnon SE, Gu XM, Kobayashi J, Kuzon WM, Jr. Force deficits in skeletal muscle after delayed reinnervation. Plastic and Reconstructive Surgery. 2004; 113: 1712–1718.
[7] Terzis JK, Tzafetta K. The "babysitter" procedure: minihypoglossal to facial nerve transfer and cross-facial nerve grafting. Plastic and Reconstructive Surgery. 2009; 123: 865–876.
[8] Terzis JK, Tzafetta K. "Babysitter" procedure with concomitant muscle transfer in facial paralysis. Plastic and Reconstructive Surgery. 2009; 124: 1142–1156.
[9] Sulaiman OAR, Gordon T. A rat study of the use of end-to-side peripheral nerve repair as a "babysitting" technique to reduce the deleterious effect of chronic denervation. Journal of Neurosurgery. 2018; 131: 622–632.
[10] Ueda K, Akiyoshi K, Suzuki Y, Ohkouchi M, Hirose T, Asai E, *et al.* Combination of hypoglossal-facial nerve jump graft by end-to-side neurorrhaphy and cross-face nerve graft for the treatment of facial paralysis. Journal of Reconstructive Microsurgery. 2007; 23: 181–187.
[11] Sleilati FH, Nasr MW, Stephan HA, Asmar ZD, Hokayem NE. Treating facial nerve palsy by true termino-lateral hypoglossal-facial nerve anastomosis. Journal of Plastic, Reconstructive & Aesthetic Surgery. 2010; 63: 1807–1812.
[12] Ding C, Hammarlund M. Mechanisms of injury-induced axon degeneration. Current Opinion in Neurobiology. 2019; 57: 171-178.
[13] Li QT, Zhang PX, Yin XF, Han N, Kou YH, Deng JX, *et al.* Functional recovery of denervated skeletal muscle with sensory or mixed nerve protection: a pilot study. PLoS ONE. 2013; 8: e79746.
[14] Li Q, Zhang P, Yin X, Han N, Kou Y, Jiang B. Early sensory protection in reverse end-to-side neurorrhaphy to improve the functional recovery of chronically denervated muscle in rat: a pilot study. Journal of Neurosurgery. 2014; 121: 415–422.
[15] Li Q, Zhang P, Yin X, Jiang B. Early nerve protection with anterior interosseous nerve in modified end-to-side neurorrhaphy repairs high ulnar nerve injury: a hypothesis of a novel surgical technique. Artificial Cells, Nanomedicine, and Biotechnology. 2015; 43: 103–105.
[16] Bodine SC, Latres E, Baumhueter S, Lai VK, Nunez L, Clarke BA, *et al.* Identification of ubiquitin ligases required for skeletal muscle atrophy. Science. 2001; 294: 1704–1708.
[17] Bodine SC, Stitt TN, Gonzalez M, Kline WO, Stover GL, Bauerlein R, *et al.* Akt/mTOR pathway is a crucial regulator of skeletal muscle hypertrophy and can prevent muscle atrophy *in vivo*. Nature Cell Biology. 2001; 3: 1014–1019.
[18] Rommel C, Bodine SC, Clarke BA, Rossman R, Nunez L, Stitt TN, *et al.* Mediation of IGF-1-induced skeletal myotube hypertrophy by PI(3)K/Akt/mTOR and PI(3)K/Akt/GSK3 pathways. Nature Cell Biology. 2001; 3: 1009–1013.
[19] Thoreen CC, Chantranupong L, Keys HR, Wang T, Gray NS, Sabatini DM. A unifying model for mTORC1-mediated regulation of mRNA translation. Nature. 2012; 485: 109–113.
[20] Ilha J, do Espírito-Santo CC, de Freitas GR. MTOR signaling pathway and protein synthesis: from training to aging and muscle autophagy. Advances in Experimental Medicine and Biology. 2018; 1088: 139–151.
[21] Yoon M. MTOR as a key regulator in maintaining skeletal muscle mass. Frontiers in Physiology. 2017; 8: 788.
[22] Pigna E, Sanna K, Coletti D, Li Z, Parlakian A, Adamo S, *et al.* Increasing autophagy does not affect neurogenic muscle atrophy. European Journal of Translational Myology. 2018; 28: 7687–7687.
[23] Tang H, Inoki K, Brooks SV, Okazawa H, Lee M, Wang J, *et al.* MTORC1 underlies age-related muscle fiber damage and loss by inducing oxidative stress and catabolism. Aging Cell. 2019; 18: e12943.
[24] Tang H, Inoki K, Lee M, Wright E, Khuong A, Khuong A, *et al.* MTORC1 promotes denervation-induced muscle atrophy through a mechanism involving the activation of FOXO and E3 ubiquitin ligases. Science Signaling. 2014; 7: ra18.
[25] Liu F, Zhang H, Zhang K, Wang X, Li S, Yin Y. Rapamycin promotes Schwann cell migration and nerve growth factor secretion. Neural Regeneration Research. 2014; 9: 602–609.
[26] Ding T, Zhu C, Yin JB, Zhang T, Lu YC, Ren J, *et al.* Slow-releasing rapamycin-coated bionic peripheral nerve scaffold promotes the regeneration of rat sciatic nerve after injury. Life Sciences. 2015; 122: 92–99.
[27] Jiang BG, Yin XF, Zhang DY, Fu ZG, Zhang HB. Maximum number of collaterals developed by one axon during peripheral nerve regeneration and the influence of that number on reinnervation effects. European Neurology. 2007; 58: 12–20.
[28] Nicks J, Lee S, Harris A, Falk DJ, Todd AG, Arredondo K, *et al.* Rapamycin improves peripheral nerve myelination while it fails to benefit neuromuscular performance in neuropathic mice. Neurobiology of Disease. 2014; 70: 224–236.
[29] Bain JR, Mackinnon SE, Hunter DA. Functional evaluation of complete sciatic, peroneal, and posterior tibial nerve lesions in the rat. Plastic and Reconstructive Surgery. 1989; 83: 129–138.
[30] Veltri K, Kwiecien JM, Minet W, Fahnestock M, Bain JR. Contribution of the distal nerve sheath to nerve and muscle preservation following denervation and sensory protection. Journal of Reconstructive Microsurgery. 2005; 21: 57–70.
[31] Noordin S, Ahmed M, Rehman R, Ahmad T, Hashmi P. Neuronal regeneration in denervated muscle following sensory and muscular neurotization. Acta Orthopaedica. 2008; 79: 126–133.
[32] Baron A, Strohl A. Severe cubital tunnel syndrome: considerations for nerve transfer surgery. Current Reviews in Musculoskeletal Medicine. 2020; 13: 708–716.
[33] Wang Y, Meng D, Zhang J, Jiang L, Xu Q, Chen Z, *et al.* Efficacy and safety of the babysitter procedure with different percentages of partial neurectomy. Annals of Plastic Surgery. 2017; 79: 286–292.
[34] Rafuse VF, Gordon T, Orozco R. Proportional enlargement of motor units after partial denervation of cat triceps surae muscles. Journal of Neurophysiology. 1992; 68: 1261–1276.
[35] Tam SL, Archibald V, Jassar B, Tyreman N, Gordon T. Increased neuromuscular activity reduces sprouting in partially denervated muscles. Journal of Neuroscience. 2001; 21: 654–667.
[36] Kamei Y, Miura S, Suzuki M, Kai Y, Mizukami J, Taniguchi T, *et al.* Skeletal muscle FOXO1 (FKHR) transgenic mice have less skeletal muscle mass, down-regulated Type I (slow twitch/red muscle) fiber genes, and impaired glycemic control. Journal of Biological Chemistry. 2004; 279: 41114–41123.
[37] Bonaldo P, Sandri M. Cellular and molecular mechanisms of muscle atrophy. Disease Models & Mechanisms. 2013; 6: 25–39.
[38] Sandri M, Coletto L, Grumati P, Bonaldo P. Misregulation of autophagy and protein degradation systems in myopathies and muscular dystrophies. Journal of Cell Science. 2013; 126: 5325–5333.
[39] Dutt V, Gupta S, Dabur R, Injeti E, Mittal A. Skeletal muscle atrophy: potential therapeutic agents and their mechanisms of action. Pharmacological Research. 2015; 99: 86–100.
[40] Rom O, Reznick AZ. The role of E3 ubiquitin-ligases MuRF-1 and MAFbx in loss of skeletal muscle mass. Free Radical Biology & Medicine. 2016; 98: 218–230.
[41] Castets P, Rion N, Théodore M, Falcetta D, Lin S, Reischl M, *et al.* mTORC1 and PKB/Akt control the muscle response to denervation by regulating autophagy and HDAC4. Nature communications. 2019; 10: 3187.